Heart rate variability analysis

PDSB 2019 – Group 1
André Miranda - 83811
Rafael Correia – 83828

Abstract

Over the years, many correlations were made between the autonomic nervous system and cardiovascular mortality and morbidity. This motivated the development of quantitative indicators of autonomic activity, such as measures of Heart Rate Variability (HRV), which describes changes over time in the interval between consecutive heart beats. HRV is modulated by several physiological mechanisms, the main one being the balance between the activity of the sympathetic and parasympathetic nervous systems. HRV parameters aim at characterizing large amounts of ECG data in an effort to identify patterns and abnormalities with clinical significance. However, due to the complexity of HRV, a lack of significant clinical correlations exists for some of these measures. Additional clinical data and HRV research tools may help establish such correlations. The present work led to the development of a programme for the analysis of HRV (called HRV Metrics). For a given ECG record it reports back several types of parameters such as time- and frequency- domain metrics as well as non-linear metrics.

Keywords: Heart rate variability, ECG, Measuring methods, Sympathovagal influences, R-peak detection, MIT database

1. PROBLEM AND MOTIVATION

There are many challenges when trying to compute HRV metrics. First of all, the QRS complex peaks must be found in order to calculate the RR intervals. Many algorithms that search for these peaks have been presented in the literature [1][2][3][4][5] with different degrees of sensitivity. In this work we elaborate on the algorithm described by P. Kathirvel et al [6]. Their work is based on a new nonlinear transformation and First-Order Gaussian Differentiator and outperforms other existing algorithms where complex QRS morphologies are present. Here, the authors try to implement and improve the algorithm where possible.

Another problem is that many HRV parameters are not yet correlated with the health state of patients. Such uncorrelated parameters include, although not limited to, entropy metrics such as sample entropy, approximate entropy or MSE which measure the complexity or irregularity of the signal [7]. Therefore, several of the available HRV metrics do not help in clinical diagnostics because they are not related to any specific disease or condition. Investigation plays a key role here, but scientists cannot study these correlations without data. Hence, databanks, where both HRV records, its metrics and patient conditions are present are essential for further development of this field. The development of the programme that resulted from this work is an important step towards the creation of these databanks as, assuming the use of the program as a standard for clinical practice, it will allow doctors to issue reports containing the mentioned necessary data.

This will allow validation of new HRV parameters and actual clinical use for those parameters which correlations to health conditions are already known.

2. BACKGROUND AND RELATED WORK

Heart Rate Variability (HRV) refers to the change over time of the periods between consecutive heart beats. HRV is thought to depend on many different physiological factors affecting the normal heart rhythm, namely autonomic neural regulation and baroreceptor reflex. Variations in the beat to beat interval of a healthy subject's heart can be highly complex and non-linear. In a clinical setting, HRV analysis relies on studying the heart's ability to adapt to different stimuli. While changes in HRV have been correlated with different pathologies, it is in cardiovascular mortality and morbidity that HRV excels as a predictor of disease. However, HRV alone is not enough to support a clinical diagnosis since HRV changes are not specific to a certain disease. It should also be noted that HRV measurements are non-invasive, easy to perform with the proper software and have good reproducibility under standardized norms.

2.1 Physiology of the ECG signal

Heart Rate Variability reflects the activity of the human heart. This organ guarantees the distribution of nutrients and oxygen throughout the body, acting as a pump that pushes blood. To do this, the heart, made up of muscle tissue, relies on a periodical electrical discharge to contract in a coordinated way. As a consequence of this discharge, by attaching two electrodes to the chest of the patient, it is possible to measure changes in electrical potential during the cardiac cycle. The resulting signal is an ECG (Electrocardiogram).

In a healthy subject, each cardiac cycle begins with the stimulation of the sinoatrial (SA) node. This node is situated in the right atrium, resulting in the local depolarization of the heart muscle. The SA node is considered the natural pacemaker of the heart, being stimulated regularly at a frequency of around 100 to 120 beats per minute (bpm). After depolarizing both the right and left atria, the electrical impulse arrives at the atrioventricular (AV) node. In regular circumstances, the propagation of the electrical stimulation to the ventricles of the heart is only possible through the AV node, which delays the conduction of the electrical stimulus momentarily to prevent abnormally fast atrial impulses.

Following the passage through the AV node, the electrical stimulus is then led to the bundle of His which distributes the signal to both ventricles. After ventricle depolarization refractory period occurs for more than 200 ms. During this period, the ventricles are unable to contract again. Subsequently, the ventricles repolarize and recover their resting electrical potential, allowing the heart to repeat its cycle.

2.1.1 ECG Waveform

A typical ECG waveform is composed by an initial P-wave, caused by the depolarization of the atria. This is followed by a QRS

complex which is the portion of the ECG with the largest amplitude and a peak like appearance, corresponding mainly to ventricle depolarization and to a lesser degree to the repolarization of the atria. Finally, ventricle repolarization originates a T-wave. Although a typical ECG has these distinguishable waves, these may sometimes merge or have varying amplitudes between each other, a fact that may be present in healthy subjects, as ECG's morphology can vary substantially between patients or even in the same patient if the electrodes are placed in a different configuration. Some known measures related with the ECG are the average heart rate (HR_{60}), calculated by counting the number of heartbeats in a 60 second window. On the other hand, instantaneous heart rate, HR_i, is obtained by dividing 60 by the time in seconds between consecutive QRS peaks (also known as an RR interval). HR_{60} may vary from 30 to 220 bpm.

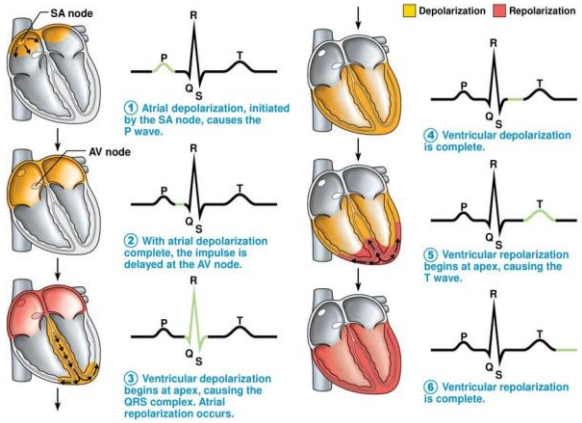

Figure 1 - Stages of ECG waveform formation

2.1.2 Ectopic Beats

Although a great majority of heartbeats occur at regular but slightly varying intervals of similar morphology, beats may happen prematurely in the cardiac cycle. These are known as ectopic beats and their morphology is different than that of the regular beats. It has been recently discovered that individuals with a higher than normal number of ectopic beats may be at an increased risk of fatal arrythmias or other cardiovascular diseases or having a poor recovery after a traumatic heart event.

A beat is classified as an ectopic beat when its R-peak occurs roughly 20% earlier than the previous beat. This may originate from electrical signals from any region of the heart other than the SA node, and are usually categorized has atrial, ventricular or prevenient from the AV node.

2.2 Factors influencing HRV

A person's heart rate (HR_{60}) is dependent on many intrapatient and interpatient factors. Intrapatient factors may include the degree of physical effort or psychological distress a person is undergoing at the time. Interpatient factors comprise genetic reasons, sex, age, medical condition and level of fitness. Even if HR_{60} is kept constant during a given period of time, instantaneous RR interval or HR_i are likely to oscillate around the mean value of HR_{60}. This phenomenon, defined before as HRV, was deemed clinically relevant in the context of fetal distress, since changes in RR interval patterns would occur before a significant difference was noted in fetal baseline heart rate [8]. Some regulators of HR and HRV will now be described.

2.2.1 Sympathovagal Balance

The central nervous system is responsible for controlling the voluntary motor system as well as the autonomic nervous system (ANS) which regulates internal organs such as the heart, lungs, digestive track and many other functions which humans don't consciously do. ANS can be split into the parasympathetic nervous system (PNS) and sympathetic nervous system (SNS). The PNS regulates mechanisms mainly related with rest and digest functions. It commonly causes a decrease in HR and blood pressure (BP) and an increase in the activity of the digestive system. On the other hand, the SNS handles stressful situations both physical and mental. It is also commonly known as the "fight of flight" response system, being related with an increase in HR, cardiac output and blood flow being directed from the digestive system to the muscles.

While parasympathetic and sympathetic stimulations do not have a direct effect on the SA node discharge frequency, they do change its sensitivity of discharge in a competing manner. Heart cells rely on two types of receptors one related with the PNS and the other with the SNS, respectively, acetylcholine and norepinephrine, that depending on the activation level excite or inhibit proteins responsible for regulating the calcium in the heart's membrane. The calcium is, in turn, what dictates HR and strength of contraction [9][10].

The parasympathetic stimulus response has a latency period of roughly 400 ms and its influence in the heartbeat has a short duration. On the contrary, the effect of sympathetic stimulation has a delay of up to 5 s after onset but is followed by an increase in HR that can last up to 30 s [11]. Therefore, it seems natural that rhythmic contributions from SNS and PNS control the RR intervals at different frequency bands.

2.2.2 HRV Frequency Domain

SNS activity ranges between 0.04-0.15Hz commonly mentioned as low frequency band (LF). On the other hand, PNS activity is associated with frequencies in the range 0.15-0.4Hz, also known as high frequency band (HF). The spectral analysis of HRV is split into different frequency bands because it is assumed that different biological regulatory mechanisms linked to HRV are limited to these. Besides the bands previously mentioned, the spectrum also includes ultra-low frequencies (ULF) in the range < 0.003Hz; and very low frequencies (VLF) in the range 0.003-0.04Hz [12].

ULF comprise oscillations with a period of 5 minutes to 24 hours (< 0.003Hz) and require the patient to be monitored for at least 24 hours [12]. The mechanisms behind ULF have not yet been determined but they consist of very slow-acting biological processes such as circadian rhythms, body temperature, renin-angiotensin system and metabolism in general.

VLF contains frequencies with a period of 25 seconds to 5 minutes (0.003-0.04Hz), thus demanding a recording period of 5 minutes or more. The main physiological mechanism thought to regulate VLF is the heart's intrinsic nervous system with SNS taking a part in this regulation. However, SNS blockage does not affect VLF power but PNS activity does, suggesting PNS may also contribute to VLF. Other factors influencing VLF may include physical activity, body temperature and renin-angiotensin system. Clinically, VLF power is more correlated with mortality than LF or HF power. Low VLF power has been associated with high inflammation, PTSD and arrhythmic death [12][13][14].

LF band includes frequencies between 0.04-0.15Hz, that is oscillations with a period between 7 seconds and 25 seconds. This band may be recorded over a period of 2 minutes. While some

authors associate LF band with SNS activity, this is not solely the case. Indeed, it may also reflect PNS activity and largely baroreceptor activity, especially when the patient is in resting conditions. When slow respiration rates are present (3-9 cycles per minute), vagal activity can influence HRV rhythms in the LF band [12][15][16].

Lastly, to HF band belong frequencies between 0.15-0.40Hz, which can be identified in ECG recordings of over 1 minute. HF band reflects parasympathetic activity related with the respiratory cycle and the RSA mechanism. Vagal blockage was reported to significantly impair HF oscillations and reduce LF band power. HR rises during inspiration and decreases with expiration, since vagal cardiovascular activity is inhibited during inhalation. The lack of vagal inhibition during inhalation was associated with increased morbidity. Besides, lower HF power has been correlated with anxiety and stress [12][15][17].

2.2.3 Clinical Relevance

The heart's SA node without ANS regulation would cause a HR_{60} of 100 to 120 bpm. Nevertheless, in healthy individuals, the effects of PNS and SNS leave a resting human with a HR_{60} of 70 to 80 bpm, since both systems always have a baseline activity; and depending on physical activity may go all the way up to 200 bpm.

The parasympathetic and sympathetic systems are constantly influenced by many factors related with cardiovascular and central nervous system (CNS). Their balance modulates HR as well as HRV. One major factor determining SNS-PNS balance is the stimulation of baroreceptors in the walls of some arteries, which causes a rise in parasympathetic (or vagal) activity and a decrease in sympathetic activity, resulting in a decrease in HR. Baroreceptors stimulation is linked to an increase in blood pressure (BP) since this will stretch the vessel walls, causing the discharge of baroreceptors. Conversely, a decrease in BP will cause the heart rate to increase [11].

Another factor influencing HR and its variability is Respiratory Sinus Arrhythmia (RSA), a phenomenon commonly seen even in healthy subjects, consisting on the acceleration of HR_i (shortening of RR intervals) on inspiration and a decrease in HR_i during expiration. RSA is influenced by variations in intrathoracic pressure, which decreases during inspiration reducing the activity of the parasympathetic system. Consequently, HR increases. Furthermore, a decrease in the amount of blood reaching the right atria causes an increase in HR. In general, the degree of RSA shows a linear relation with parasympathetic cardiovascular control and is attenuated at later ages [18][19].

Exercise is also known to increase HR due to a reduction in vagal activity and an increase in sympathetic activity which vasoconstricts non used muscles and internal organs that do not have an important function in the stressful response. While, in the short term, exercising increases HR, training leads to a long term lower resting HR and a higher maximum HR. It has also been found that aerobic athletes have increased power in all HRV frequency bands. Elevated cholesterol levels are commonly associated with lower HRV.

Heart Rate Variability declines with age, predominantly in males, while also being low in young children [20]

Circadian rhythms also partake in SNS-PNS balance with a decline in BP and HR during sleep, and also having effects during the day, depending on the subject level of awareness and circulating hormone concentration [21]. Compared to non-REM sleep, there was an increase in power of the spectral analysis in REM sleep. This power level increased with each REM sleep cycle and was more noticeable in the VLF and LF spectral components. In patients with sleep apnea, a spectral peak, corresponding to the recurrence rate of apnea, can be noticed somewhere in VLF and LF bands [22][23].

HRV analysis can easily detect imbalances between SNS and PNS which are commonly present in patients with psychiatric disorders. Furthermore, regular oscillations in HR are reduced in patients with severe brain damage and depression [24][25].

Clinically, HRV can be used as a predictor of cardiovascular disease, with reduced HRV being used as a measure of chronic heart failure associated with autonomic disfunction. Patients at a higher risk of death due to progressive heart failure usually have lower HRV. Furthermore, clinical evidence points towards a decrease in vagal activity in favor of sympathetic dominance after myocardial infarction, especially in more serious cases where a lower HRV can be predictive of a higher rate of mortality or arrhythmic complications, and a lower chance of recovery in general. Low vagal activity and high sympathetic activity decreases the fibrillation threshold, predisposing a patient to ventricular fibrillation. A lower HRV is also linked with sudden cardiac death or ventricular tachycardia. Regarding myocardial disfunction, in advanced phases of the disease, there's a drastic reduction in HRV with very low LF component, resulting from the fact that the sinus nodes loses responsiveness to neural inputs. HRV was found to be significantly reduced in patients with left ventricular hypertrophy (LVH) caused by hypertension or aortic valve disease [26][27] [28][29]. Beta blockers may be able to restore balance to SNS and PNS in cardiovascular diseases by restricting the sympathetic dominance that usually exists [30].

In diabetic patients a reduction in HRV due to parasympathetic activity withdrawal usually precedes the clinical appearance of autonomic neuropathy [31].

In patients with renal failure spectral analysis showed reduction in the HR power spectrum at all frequency bands, accentuated in the HF band corresponding to PNS impairment [32].

Studies showed that smoking reduces HRV by increasing sympathetic activity in detriment of vagal activity [33]. In case of acute alcohol ingestion HRV is reduced and in cases of chronic alcohol dependence, vagal neuropathy was found in men [34].

Although higher HRV is usually correlated with better clinical outcomes, extreme values of HRV can be linked to issues such as atrial fibrillation. HRV should be kept around optimal levels proven to demonstrate a healthy adaptability to regulatory stimuli.

In the present work, various parameters were included. Some examples of such metrics are the time-domain parameters: standard deviation of the NN intervals, SDNN, the standard deviation of the difference between adjacent NN intervals, SDSD, the root mean square of the intervals between adjacent NN intervals, RMSSD, the number adjacent intervals that differ more than 50ms, NN50, or its percentage, pNN50. SDNN has been proven useful in the stratification of cardiac risk in patients in 24h ECG recordings. Patients with SDNN values of 50ms or less were classified as unhealthy, between 50-100ms were considered to have compromised health, and above 100ms were healthy. Following heart attack, patients with SDNN under 50ms had 5.3 times higher risk of mortality in an approximate 3 year follow up period than those with SDNN over 100ms [11][12]. SDANN correlates with ULF band power [13]. SDNNI, calculated by taking the mean of the standard deviations of all the NN intervals for each 5 min segment of a 24h ECG recording, correlates with VLF band power [13].

The value of pNN50 was found to be correlated with RMSSD and PNS activity, mainly expressed in the HF band power, reflecting short term HRV [12]. Both pNN50 and RMSSD are calculated based on NN interval differences and therefore are considerably unaffected by trends present in long recordings. RMSSD is similar to the non-linear parameter SD1. Lower RMSSD was associated with a higher risk of sudden unexplained death in epilepsy patients [13][14].

HRV triangle index (HTI) is a measure of the area of the RR interval histogram divided by its height. HTI > 20.42 identifies arrhythmic patients [15].

3. APPROACH AND UNIQUENESS

3.1 Material

All ECG records used for both assessing the quality of the peak-detection algorithm and developing and testing the software were retrieved from the MIT-BIH database. This is a well-known and widely used database to verify ECG-related algorithms' performance. The database contains 48 signals from 47 different subjects which include a two-channel half-hour ECG recording. In this work, channel two was used since the derivation for that channel enhances QRS complexes, a choice that would naturally be done in clinical practice.

About half of the recordings present in the database include less common but clinically significant arrhythmias that would not be well-represented in a small random sample which is perfect to test the robustness of algorithms. All ECG recordings are sampled at 360Hz and were annotated by two or more independently cardiologists with all disagreements resolved (there are around 110.000 annotations in the database).

The ECG records from this database include signals with acceptable quality, sharp and tall P and T waves, negative QRS complex, small QRS complex, wider QRS complex, muscle noise, baseline drift, sudden changes in QRS amplitudes, sudden changes in QRS morphology, multiform premature ventricular contractions (PVCs), long pauses and irregular heart rhythms. Some authors decide to remove certain ECG records because of some unwanted features. In this work, however, the authors choose to maintain all records in the analysis for an easier comparison with past and future works.

3.2 Methods

As mentioned above, the authors tried to implement the peak-detection algorithm described by P. Kathirvel et al [6] and then improve it whenever possible. The full correct implementation was not possible since no snippets of source code were provided, and all the implementation was done relying on the descriptions of the paper which were not thorough enough. After implementing the algorithm with the greatest similarity possible the authors tried to improve the algorithm by inserting heuristics that improved the sensitivity of the algorithm.

After de work on the peak-detection algorithm, a software for the analysis of HRV was also built. The programme was called HRV Metrics and can be used both in investigation and clinical practice.

3.2.1 Peak-detection algorithm

The basic structure of the algorithm presented by P. Kathirvel et al is depicted in Figure 2. Here, a succinct description of the algorithm is made but a more detailed explanation can be found in their paper.

The algorithm comprises four stages: QRS enhancement and noise reduction, a nonlinear transformation, a peak location estimation process and the true R-peak detection.

The first step is a bandpass filter from 5Hz to 20Hz which not only eliminates the grid power noise (50Hz or 60Hz in the US) but also enhances the fast varying QRS complexes. Then, a first order differentiation step occurs, where the output signal, $d(n)$, is calculated as:

$$d[n] = f[n+1] - f[n]$$

This step dampens the effect of large P and T waves and restricts in time the effect of the R peak.

The next step is the squaring to get a positive-valued signal and further enhance prominent R peaks (compared with T or P waves). Then, an adaptative threshold based on the signals' power is performed on the squared signal to remove spurious noise spikes which effectively reduces the number of false positive detections.

Because squaring introduces large differences between R-peak amplitudes, the next step presented in the algorithm is to apply a Shannon energy transformation which results in a more uniform R-peak amplitude. The signal is then enveloped to aggregate spikes belonging to the same R-peak into one single short wave corresponding to one R-peak.

Next, a first order Gaussian differentiator (FOGD) is used to find R-peak location candidates. An M-point Gaussian curve (w) and the FOGD (w_d) are calculated as:

$$w[m] = \exp\left(-\frac{1}{2}\frac{\left(m-\frac{M}{2}\right)^2}{\sigma^2}\right), \qquad m = 1, 2, \dots, M$$

$$w_d[m] = w[m+1] + w[m], \qquad m = 1, 2, \dots, M-1$$

Figure 3 shows the two curves, w and w_d.

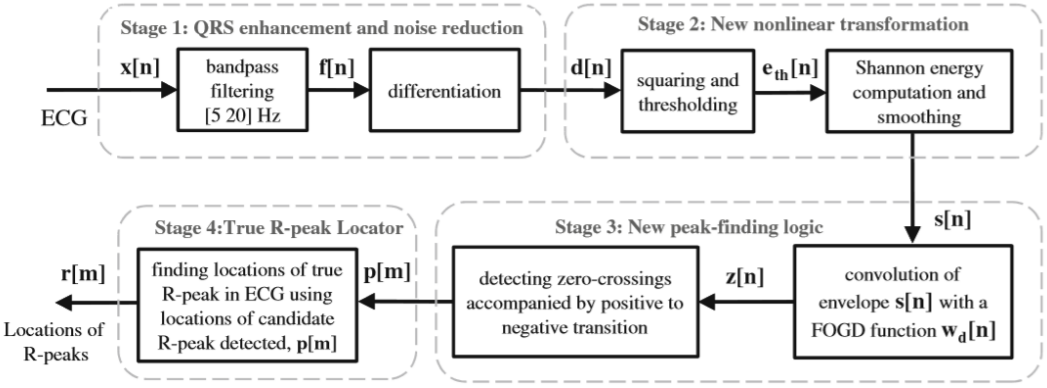

Figure 2 - Block diagram of the R-peak detection algorithm presented by P. Kathirvel et al

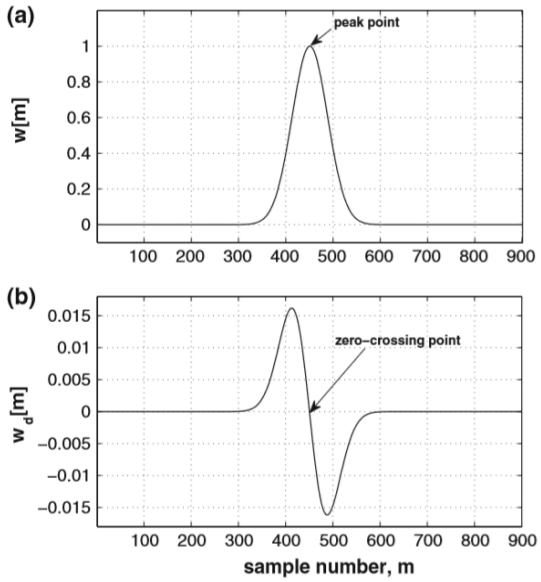

Figure 3 - Gaussian window (top) and FOGD (below)

To detect the candidate R-peaks, a discrete convolution is done between the Shannon energy envelope and the FOGD curve:

$$z[n] = \sum_{k=-\infty}^{\infty} w_d[k]s[n-k]$$

The locations at where z goes from positive to negative are selected as candidates for R-peaks. These are only candidates because there are slight time shifts due to the convolution and thus, the real peak location must be found using another step.
To find the real peak location, a window centred around the candidate is extracted from the original ECG. Then, the real peak is selected as the maximum value from that window, hoping that it corresponds to the real R-peak. This process is repeated for the candidates to gather all the R-peaks from the ECG.

On top of the presented algorithm three additional heuristics were added to improve sensitivity, which are presented next.
Firstly, before feeding the input ECG into the bandpass filter, a zero-mean detrending was performed. This was done to ensure that the bandpass filter transient at the beginning and end of the signal would not affect and obscure existing R-peaks close to the signal extremes. Also, after this step, the signal was normalized, which, in principle does not affect the preceding algorithm but confers consistence among ECG records with different amplitudes.
Secondly, before squaring, the negative values of the signal were truncated to zero. This prevented prominent negative waves that do belong to the QRS complex to be detected at the end as a false positive. Since squaring enhances both negative and positive high amplitude peaks, these are both perceived as the same type of peak and later equalized by the Shannon energy transformation. The truncation was done as:

$$tr[n] = \begin{cases} 0, & f[n] < 0 \\ f[n], & f[n] \geq 0 \end{cases}$$

Lastly, a modification is done in the step where the true peaks are searched based on the found candidates. The window centred around the candidate is extracted from the ECG signal from where the real R-peak is attributed to the local maximum. However, many are the cases when the ECG signal is not ideal both in noise and morphology. Because the signal after the bandpass is much more noise-free it presents a better comparison term from where the true R-peak can be obtained and was, hence, used.
The implementation of these three heuristics significantly improved the sensitivity of the algorithm as shown in the Results section.

3.2.2 HRV Metrics software

The programme developed is now detailed in this chapter. The goal was to obtain a friendly user interface which was intuitive to use. The Graphical User Interface (GUI) consists of several tabs that provide different functionalities. The Load tab allows the user to upload an ECG record and displays information about the file (name, number of channels, record size, etc). It also allows the selection of some time period from which the signal will be analysed (if not specified, the entire signal will be analysed).
The second tab is aimed at detecting the peaks of the uploaded ECG record and providing some information about the detected peaks such as the number of peaks, the average and the standard deviation of the beats per minute.
The next tab uses the detected peaks to construct a tachogram, the plot of the RR intervals, and a plot of the heart rate which follows an inverse relationship to the tachogram. Here, outlier's removal is also possible with different methods. The majority of the outliers coincide with ectopic beats which were described in the section 2.1.2. An instance of this tab is shown in Figure 4.

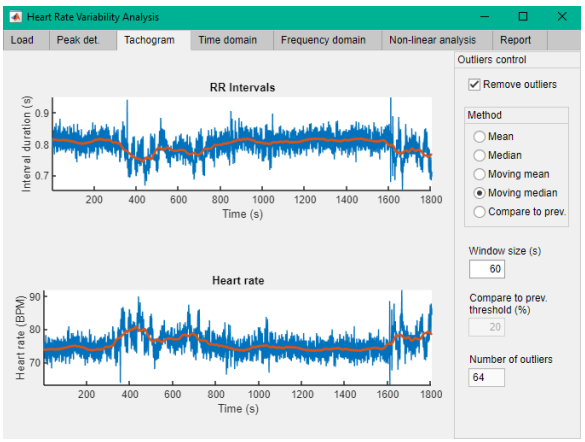

Figure 4 - Tachogram tab displaying the RR intervals plot and the heart rate monitoring

The three tabs that follow are all part of the HRV analysis, which include both time- and frequency- domain analysis and non-linear analysis. The time domain analysis tab presents two types of parameters. Statistical parameters include SDNN, SDSD, RMSSD, NN50 or pNN50. Geometric parameters give information about the geometry of the NN intervals' histogram and the exponential decay of the absolute difference between adjacent NN intervals. They include the HRV triangular index, the baseline width of the NN interval histogram, TINN, and the logarithmic index.

The frequency analysis tab is depicted in Figure 5 and allows the estimation of the power density using various methods: Lomb, auto-regressive (AR), Welch and FFT. Single or multiple power density spectrums can be displayed at any time and the spectrum metrics can be calculated based on any chosen method (in the image, Lomb method is selected to metric calculation). The frequency of the maximum spectrum value for the LF and HF frequency bands are also presented. Multiple option are available to the user such as the type of scale in which to plot the spectrograms (linear or logarithmic), the order of the AR method, the resampling interpolation method (linear or cubic; not used for Lomb method since it does not require even sampled data), the detrending order or the frequencies that define VLF, LF and HF band limits.

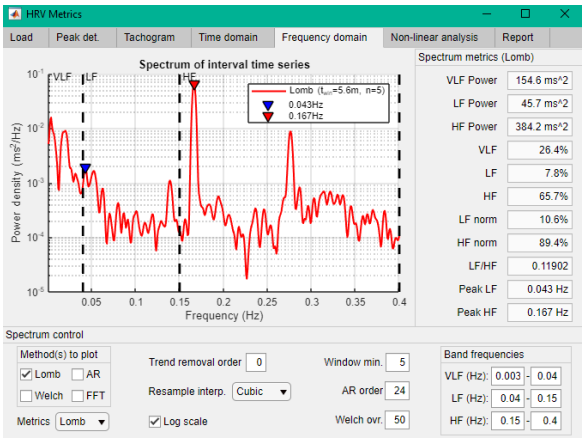

Figure 5 - Frequency analysis tab showing the power density spectrum of the uploaded ECG record.

Finally, the non-linear analysis tab is sub-divided into four other tabs, each one with one type of non-linear analysis: Poincaré plot (Figure 6), detrended fluctuations (DFA), entropy analysis and recurrence plot (Figure 7).

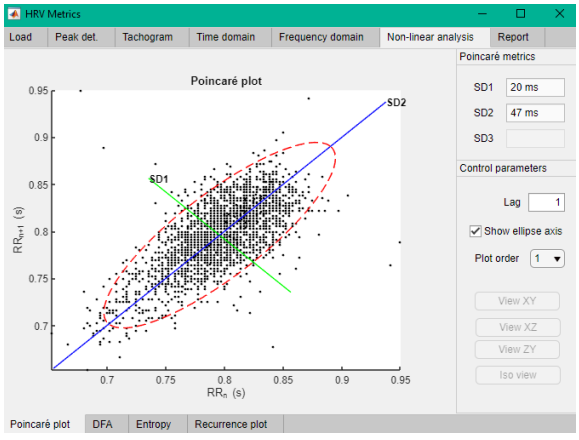

Figure 6 - Poincaré plot

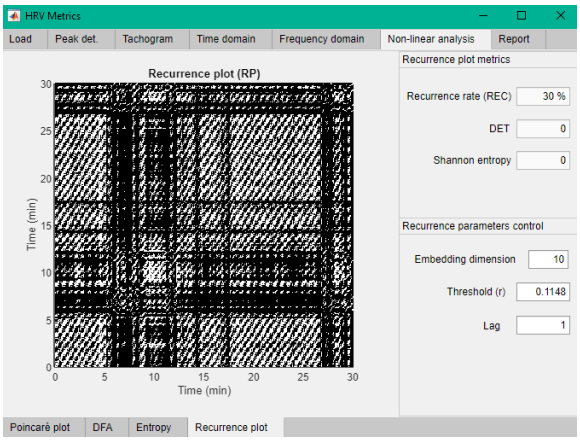

Figure 7 - Recurrence plot

4. RESULTS

4.1 Peak-detection sensitivity

In order to evaluate the reliability of the implemented peak-detection algorithm a benchmark analysis was performed. In this work, three benchmark parameters were adopted: sensitivity (S), positive predictivity (P), and detection error rate (DER). Sensitivity is the probability that a peak is detected when it is in fact present in the signal while positive predictivity specifies the percentage of correctly detected peaks compared to the total number of peaks indicated by the algorithm. These parameters are calculated by the following formulas:

$$S = \frac{TP}{TP + FN}$$

$$P = \frac{TP}{TP + FP}$$

$$DER = \frac{FP + FN}{TP}$$

, where TP is the number of true positives, FN is the number of false negatives and FP is the number of false positives. Furthermore, the overall performance of the algorithm is also computed using the detection accuracy:

$$Acc = \frac{TP}{TP + FN + FP}$$

In this work, each ECG signal was divided into 10 seconds segments (standard for data compression, transmition and storage [6]), its peaks were calculated with the proposed algorithm and compared these with the database annotations.

Since a correct peak identification does not necessarily mean returning the same sample number the verification algorithm implements a small window within which the peak detection could be present. Hence, if the absolute difference from the result and the annotation was smaller than a certain margin it would be considered as a correct peak detection. The margin was defined as 150ms since 100ms is the average width of the QRS complex found in literature [35] and to which an extra margin of 50ms was added.

The sensitivity analysis for the implemented algorithm alone and the implementation with the extra heuristics is present in Figure 8 and Figure 9, respectively. A great increase of sensitivity was achieved for some ECG records. The overall sensitivity of the

algorithm implementation alone was 89.24% while with the added heuristics a sensitivity of 99.19% was achieved.

For the implementation alone, the following values were obtained: $P = 88.95\%$, $DER = 24.48\%$, $Acc = 80.34\%$ while with the added heuristics these values are $P = 93.96\%$, $DER = 7.24\%$, $Acc = 93.25\%$, showing an improvement on all the measurements.

The sensitivity of the algorithm reported by P. Kathirvel et al was 99.94% which does not match with our results. This might be due to several factors. Firstly, the article does not provide any code source, only some pseudocode lines for the last part of the algorithm and therefore, the implementation had to be done all from scratch which inevitably introduces differences in the way it is built. Secondly, the MIT database annotations are sometimes updated which might lead to different peak-detection results, although this is not a major source of difference since these modifications are very rare and small.

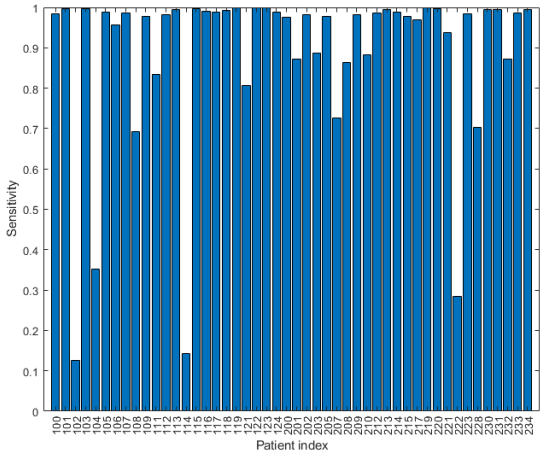

Figure 8 - Sensitivity analysis using the algorithm developed by P. Kathirvel et al depicted in Figure 2

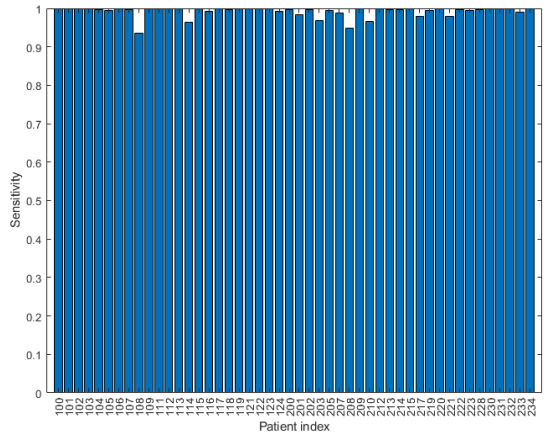

Figure 9 - Sensitivity analysis of the implemented algorithm plus the new heuristics

4.2 HRV Metrics software

The final software product achieved the initial set goals: it has a friendly-user interface which is simple and intuitive to use. The software was tested by some people that did not have any understanding of the programme and how it was designed and were only instructed to experience it. Everyone understood what the first step was supposed to be (load the ECG record), again, without any knowledge of how the software operated or what its function was. Most of the functionalities were clear and easy to use to everyone. People reported that the programme gave important feedback for the workflow of the programme such as showing warning messages when people tried to access HRV analysis tabs without uploading any ECG record.

Throughout the software, explanatory labels are presented when over hovering with the mouse, such as the meanings of HRV parameters or available options.

The last tab allows the user to automatically generate a PFD report with all the relevant information calculated by the software. An image of the report cover is shown in Figure 10.

Figure 10 - Cover of the report automatically generated from the HRV Metrics software

5. DISCUSSIONS AND CONCLUSIONS

In this work, we added a new layer of heuristics to the existing literature concerning peak-detection algorithms with a 9.95% increase in sensitivity (the final achieved sensitivity was 99.19%). This improvement was implemented in a program called HRV Metrics which after peak detection of the ECG also calculates a variety of HRV parameters.

Some of the parameters calculated in the HRV Metrics are helpful for doctors to access a patient's health status with evidence based on research , while some other parameters are still not correlated to any specific disease or conditions. The use of software tools such as the one developed int this work is a step towards the creation of databanks with information regarding HRV metrics and health status which are necessary for research purposes. The report that is automatically generated by the software is an important feature that meets the initially described motivation for it: a way to systematize knowledge about HRV parameters relating patient diseases and conditions with specific HRV metrics.

6. REFERENCES

[1] P. S. Hamilton and W. J. Tompkins, Quantitative Investigation of QRS Detection Rules Using the MIT/BIH Arrhythmia Database, *IEEE Trans. Biomed. Eng.*, vol.

BME-33, no. 12, pp. 1157–1165, 2007.

[2] X. Hongyan, H. Minsong, A new QRS detection algorithm based on empirical mode decomposition, in: Proceedings of the 2nd International Conference on Bioinformatics and Biomedical Engineering, 2008, pp. 693–696.

[3] M. Elgendi, M. Jonkman, F. De Boer, R wave detection using Coiflets wavelets, in: IEEE 35th Annual Northeast Bioengineering Conference, Boston, MA, 2009, pp. 1–2.

[4] F. Zhang, Y. Lian, QRS detection based on multi-scale mathematical morphology for wearable ECG devices in body area networks, IEEE Trans. Biomed. Circuits Syst. 3 (4) (2009) 220–228.

[5] M. S. Manikandan and K. P. Soman, A novel method for detecting R-peaks in electrocardiogram (ECG) signal, *Biomed. Signal Process. Control*, vol. 7, no. 2, pp. 118–128, 2012.

[6] P. Kathirvel, M. S. Manikandan, S. R. M. Prasanna, and K. P. Soman, An Efficient R-peak Detection Based on New Nonlinear Transformation and First-Order Gaussian Differentiator, *Cardiovasc. Eng. Technol.*, vol. 2, no. 4, pp. 408–425, 2011.

[7] Kubios, About HRV - Kubios. [Online]. Available: https://www.kubios.com/about-hrv/. [Accessed: 27-May-2019].

[8] L. S. H. E.H., Electronic evaluation of the fetal heart rate patterns preceding fetal death, *Am.J.Obstet.Gynecol.*, 1965.

[9] D. J.E, Creating Mind (How The Brain Works), *W.w.nort. Co*, 1998.

[10] M. P. L. M.N., Neural control of the heart, *Handb. Physiol.*, 1979.

[11] H. R., 'The Control and Physiological Importance of Heart Rate,' N.Y.Futura Pub.Co.Inc., 1995.

[12] M. R. Z. C. Shaffer F, 'A healthy heart is not a metronome: an integrative review of the heart's anatomy and heart rate variability,' Front Psychol, 2014.

[13] V. F. C. M. C. A. S. P. Bernardi L, 'Physical activity influences heart rate variability and very-low-frequency components in Holter electrocardiograms,' Cardiovasc Res, 1996.

[14] C. D. M. C. E. D. Taylor JA, 'Mechanisms underlying very-low-frequency RR-interval oscillations in humans,' Circulation, 1998.

[15] S. F. McCraty R, 'Heart rate variability: new perspectives on physiological mechanisms, assessment of self-regulatory capacity, and health risk,' Glob Adv Health Med, 2015.

[16] H. J. M. A. Ahmed AK, 'Respiratory control of heart rate,' Eur J Appl Physiol, 1982.

[17] T. E. Grossman P, 'Toward understanding respiratory sinus arrhythmia: relations to cardiac vagal tone, evolution and biobehavioral functions,' Biol Psychol, 2007.

[18] C. A. Malik M., 'Heart Rate Variability,' N.Y.Futura Pub.Co.Inc., 1995.

[19] M. A. P. G. B. L. La Rovere M.T., 'Baroreflex Sensitivity and Heart Rate Variability in the Assessment of the Autonomic Status,' N.Y.Futura Pub.Co.Inc.

[20] K. J. F. Y. S. D. L. M. Sinnreich R., 'Five minute recordings of heart rate variability for population studies: repeatability and age-sex characteristics,' Heart, 1998.

[21] L. P., 'The enchanted world of sleep,' Yale University Press, 1996.

[22] Y. Y. Togo F., 'Decreased fractal component of human heart rate variability during non/REM sleep,' Am.J.Physiol.Heart Cird. Physiol., 2000.

[23] D. M. e. al., 'Detection of sleep apnoea from frequency analysis of heart rate variability,' Comput.Cardiol., 2000.

[24] W. M. H. E. Lowensohn RI, 'Heart-rate variability in brain-damaged adults,' Lancet, 1977.

[25] C. R. e. al., 'Depression, heart rate variability, and acute myocardial infaction,' Circulation, 2001.

[26] N. J. e. al., 'Clinical Investigation and Reports: Prospective Study of Heart Rate Variability and Mortality in Chronic Heart Failure,' Circulation, 1998.

[27] A. A. Mc Clements BM, 'Value of signal-averaged electrocardiography, radionuclide ventriculography,Holter monitoring and clinical variables for prediction of arrhytmic events in survivors of acute myocardial infarction in the thrombolytic era,' J.Am.Coll.

[28] M. M., 'Heart Rate Variability: Standards of Measurement Physiological Interpretation, and Clinical Use,' Circulation, 1996.

[29] O. O. e. al., 'Comparison of the predictive characteristics of heart rate variavility index and left ventricular ejection fraction for all-cause mortality, arrhythmic events and sudden death after acute myocardial infarction,' Am.J.Cardiol., 1991.

[30] P. C. e. al., 'Effect of Omacor on HRV parameters in patients with recent uncomplicated myocardial infaction - a randomized, parallel group, double-blind, placebo-controlled trial:study design,' Curr Control Trials Cardiovasc Med, 2003.

[31] P. M. e. al., 'Quantitative evaluation of cardiac parasympathetic activity in normal and diabetic man,' Diabetes, 1982.

[32] C. M. M. O. Zoccali C, 'Defective reflex control of heart rate in dialysis patients: evidence for an afferent autonomic lesion,' Clin Sci, 1982.

[33] Y. M. S. Y. e. a. Hayano J, 'short, lonterm effects of cigarette somking on heart rate variability,' Am J Cardiol, 1990.

[34] M. S. e. al., 'Heart Rate Variability and cardiac autonomic function in men with chronic alcohol dependence,' Br Heart J, 1991.

[35] Normal Duration Times - Normal Function of the Heart - Cardiology Teaching Package - Practice Learning - Division of Nursing - The University of Nottingham, *The University of Nottingham*. [Online]. Available: https://www.nottingham.ac.uk/nursing/practice/resources/cardiology/function/normal_duration.php. [Accessed: 15-Jun-2019].

Author(s) Bio:

André Filipe dos Santos Miranda

Email: andre.f.s.miranda@hotmail.com

Bachelor in Biomedical Engineering at IST[1]

Erasmus semester at UT[2].

Master student in Biomedical Engineering at IST
(Imaging, Biomedical Instrumentation and Biosignals profile)

José Rafael Cabral Correia

Email: jose.rafael1997@hotmail.com

Bachelor in Biomedical Engineering at IST

Erasmus semester at UT.

Master student in Biomedical Engineering at IST
(Imaging, Biomedical Instrumentation and Biosignals profile)

[1] Instituto Superior Técnico, Lisbon (Portugal)

[2] Twente University, Enschede (Netherlands)